# Different effects of carbon and nitrogen on precipitation behavior and mechanical properties in austenitic stainless steels

**Kyung-Shik Kim, Jee-Hyun Kang, Sung-Joon Kim**

Austenitic stainless steels, which are the most common type of stainless steels have good weldability and formability, and can be used in a wide range of temperatures. However, precipitation of carbides and nitrides may have detrimental effects on their mechanical properties. Fe-15Cr-15Mn-4Ni based steels were investigated in this research with different contents of 0.2C, 0.2N and 0.2C+0.2N. Precipitation behavior was observed by aging the specimens in temperature range from 600 OC to 1000 OC for up to 240 hours. Precipitates of M23C6 and Cr2N were formed. The specimens containing 0.2% of carbon formed M23C6 along grain boundaries and within grains depending on the aging condition. Cr2N, however, was formed only at grain boundaries in the specimens containing 0.2% of nitrogen. The specimens containing both carbon and nitrogen formed both carbide and nitride, the fractions of which are different. TTP (Time-Temperature-Precipitation) diagrams were constructed based on the observation. Moreover, tensile test was conducted to identify the effect of precipitation on mechanical properties. Specimens with carbon showed more decrease in elongation and increase in ultimate tensile strength (UTS), whereas ones with nitrides showed no distinct change in elongation and UTS. The different effects of nitrogen and carbon are discussed in detail.

**KEYWORDS:** AUSTENITIC STAINLESS STEEL, PRECIPITATION, CARBIDE, NITRIDE, MICROSTRUCTURE, MECHANICAL PROPERTY

## INTRODUCTION

Austenitic stainless steels (ASSs) are widely used due to their excellent corrosion resistance, toughness and formability. 70% of stainless steel market demand is satisfied with AISI 300 series austenitic stainless steels which contain 18 wt.% of chromium and 8-12 wt.% of nickel. However, the price of nickel is high and unstable. Therefore, replacing nickel with manganese has been actively investigated. Furthermore, carbon and nitrogen are added, since both nitrogen and carbon are strong austenite stabilizers and effectively enhance the strength and corrosion resistance of material [1-2]. However, the addition of these interstitials induces the precipitation of carbides and nitrides at high temperatures [3]. Precipitates are formed at grain boundaries in most cases, which can degrade the mechanical properties of materials [4-5]. As a consequence, research on the precipitate kinetics is important for the austenitic stainless steels containing high interstitials.

Carbon and nitrogen tend to distribute differently in interstitial sites of a steel; carbon prefers to cluster, i.e. short-range decomposition, while nitrogen never locates as a first neighbor to each other, i.e. short-range ordering, when they are in solid solution. Moreover, the effect of simultaneous alloying of carbon and nitrogen is not additive, and the austenitic steel with C+N are even more stabilized than that with either carbon or nitrogen of the equivalent concentration [6-8]. Such different atomic distribution results in the stability variation of carbon and nitrogen in solid solution, which would affect the thermodynamics and kinetics of carbide / nitride precipitation.

In the present study, the precipitation behavior of manganese containing austenitic stainless steels with either carbon or nitrogen is investigated at a 600-1000 $^{0}$C temperature range. The effect of the precipitates on mechanical properties is also studied by tensile test at room temperature.

**Kyung-Shik Kim, Jee-Hyun Kang, Sung-Joon Kim**

Graduate Institute of Ferrous Technology (GIFT), POSTECH, Republic of Korea

## EXPERIMENTAL PROCEDURE

**Tab.1** - Compositions (wt%) of the samples

| CHEMICAL COMPOSITION (wt.%) | | | | | | |
|---|---|---|---|---|---|---|
| Alloy | Cr | Mn | Ni | Si | C | N |
| Base | 15.4 | 14.8 | 4.1 | 0.33 | 0.002 | 0.008 |
| C2 | 14.9 | 15.0 | 4.0 | 0.29 | 0.208 | 0.004 |
| N2 | 15.0 | 15.2 | 4.1 | 0.26 | 0.015 | 0.192 |
| CN20 | 15.1 | 15.3 | 4.0 | 0.33 | 0.210 | 0.195 |

The compositions of four alloys, in this study, Base, C2, N2 and CN20 are listed in Table 1. A 15Cr-15Mn-4Ni based steel can contain carbon and nitrogen up to 0.3 wt.% in solid solution and retain a full austenitic microstructure at room temperature. Thermodynamic calculations were carried out by MatCalc version 6.00 with mc_fe database to assess the equilibrium phases and the driving force for precipitates.

25 kg ingots of four alloys were heat treated at 1200 $^{0}$C for two hours and hot rolled to 12 mm. Plates were then cut and annealed at 1100 $^{0}$C for 30 minutes to obtain a full austenite microstructure. The grain size of austenite matrix for each alloy was 52 ± 6 μm for Base, 89 ± 5 μm for C2, 62 ± 5 μm for N2, and 56 ± 4 μm for CN20. After cutting the samples to 1.2 × 0.5 × 1.5 mm$^3$, they were aged at temperatures from 600 to 1000 $^{0}$C with a 100 $^{0}$C interval. The aging times were 10, 30, 60, 180, 600, 1440, and 14400 minutes.

Precipitates were analyzed with FE-SEM, EDS and TEM. SEM samples were prepared by mechanical polishing which was finished with colloidal silica. Back scattered electron (BSE) images were analyzed to produce time-temperature-precipitation (TTP) diagrams and to calculate the distribution of precipitate. FE-SEM EDS and TEM were employed to identify the precipitates. By detecting the different EDS signals of carbon and nitrogen in the precipitates, carbides and nitrides could be qualitatively distinguished. Detailed classification of the precipitates was performed by analyzing diffraction patterns taken by TEM. TEM specimens were prepared by jet polishing at 20.5 V with 10% perchloric acid mixed with 90% acetic acid as an electrolyte after mechanical polishing to a thickness of 100 μm.

Based on the observed precipitation behavior, tensile tests were carried out to obtain the mechanical properties. The samples aged at 800 $^{0}$C were used to clearly see the effect of the precipitates on the mechanical properties. Subsized tensile specimens with a thickness of 1.5 mm were machined according to ASTM E8M-4, and tested with constant displacement speed of 1 mm min$^{-1}$ which corresponds to an initial strain rate of 6.67 × 10$^{-4}$ s$^{-1}$.

Deformed samples were investigated by EBSD to identify their deformation mechanism. The distributions of phases and twin boundaries were observed in the samples without aging and after aging at 800 $^{0}$C for 14400 min. The EBSD samples were prepared in the same way with the XRD samples.

## RESULTS AND DISCUSSION

### 1. Precipitation behavior

Based on the observation of precipitates, TTP diagrams were constructed and shown in Fig. 1. According to the diagram, the generated precipitates largely depend on the alloy composition. Sigma phase and δ-ferrite were formed in Base, intergranular and intragranular $M_{23}C_6$ in C2, intergranular $Cr_2N$ in N2, and both $M_{23}C_6$ and $Cr_2N$ in CN20.

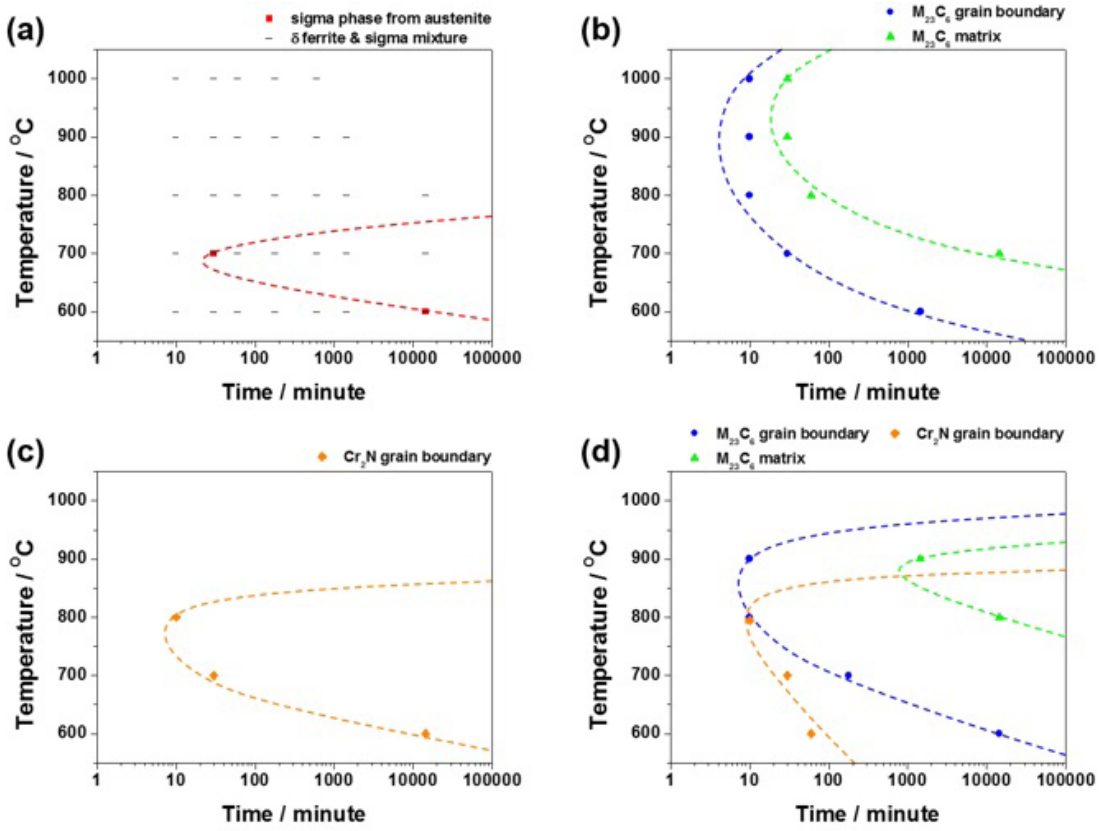


**Fig. 1** - TTP diagrams of (a) Base, (b) C2, (c) N2, and (d) CN20.

General morphologies of the precipitates after aging at 700 °C for 14400 min are shown in Fig. 2, where the dark particles in the images are the precipitates. Light elements give dark contrast in the BSE mode, and therefore, all $M_{23}C_6$, $Cr_2N$, sigma phase which are enriched with lighter elements than Fe appear darker than the austenitic matrix. These precipitates are distinguished by their selected area diffraction patterns taken by TEM. Some examples are shown in Fig. 3. Both intergranular and intragranular $M_{23}C_6$ showed orientation relationship with the austenite matrix; however, sigma and nitride particles did not show any orientation relationship.

The observed existences of different precipitates agree with thermodynamic calculation results in Fig. 4 where phase fractions of austenite, $M_{23}C_6$, $Cr_2N$, sigma, and δ-ferrite are shown according to temperature.

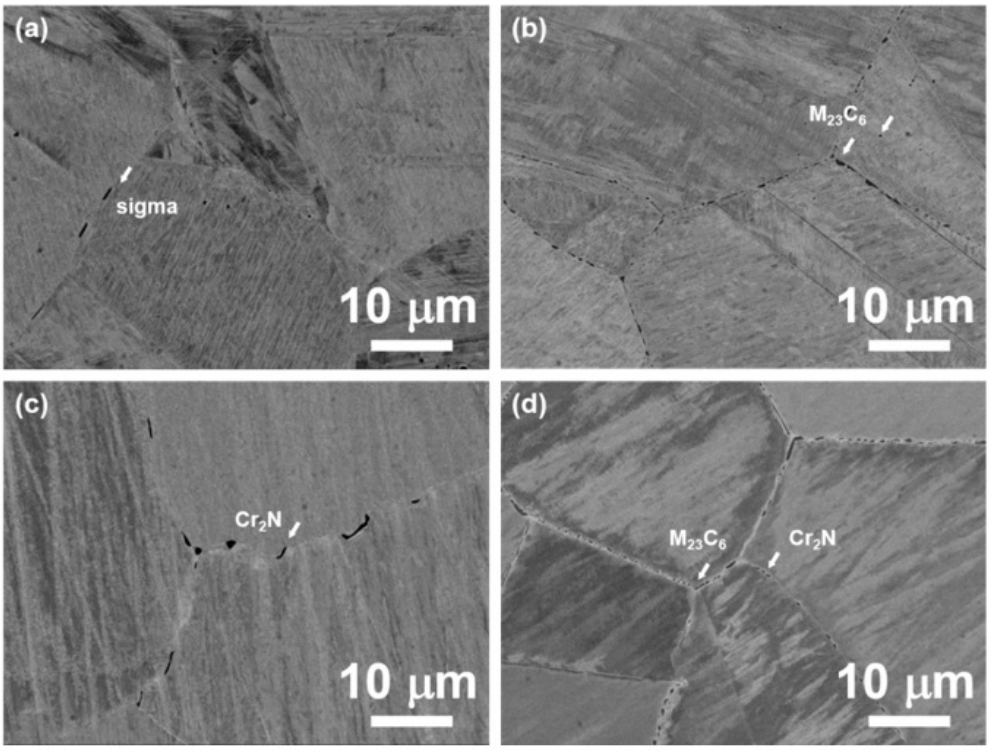


**Fig. 2** - BSE images of (a) Base, (b) C2, (c) N2, (d) CN20, aged at 700 °C for 14400 min.

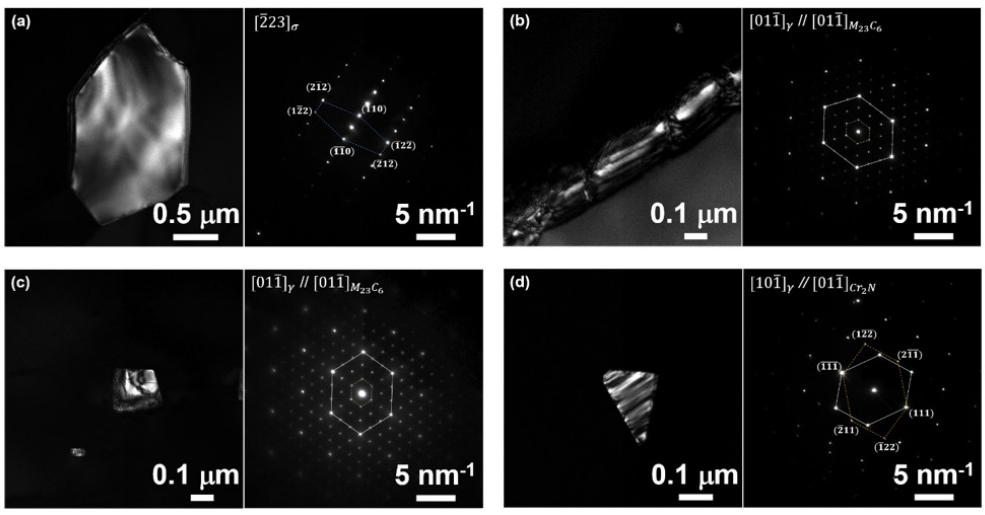


**Fig. 3** - TEM dark field image and diffraction patterns of (a) sigma phase in Base after 700°C aging, (b) grain boundary $M_{23}C_6$ and (c) intragranuluar $M_{23}C_6$ in C2 after 900°C aging, and (d) $Cr_2N$ in N2 after 700°C aging. All photos are taken after aging for 14400 min.

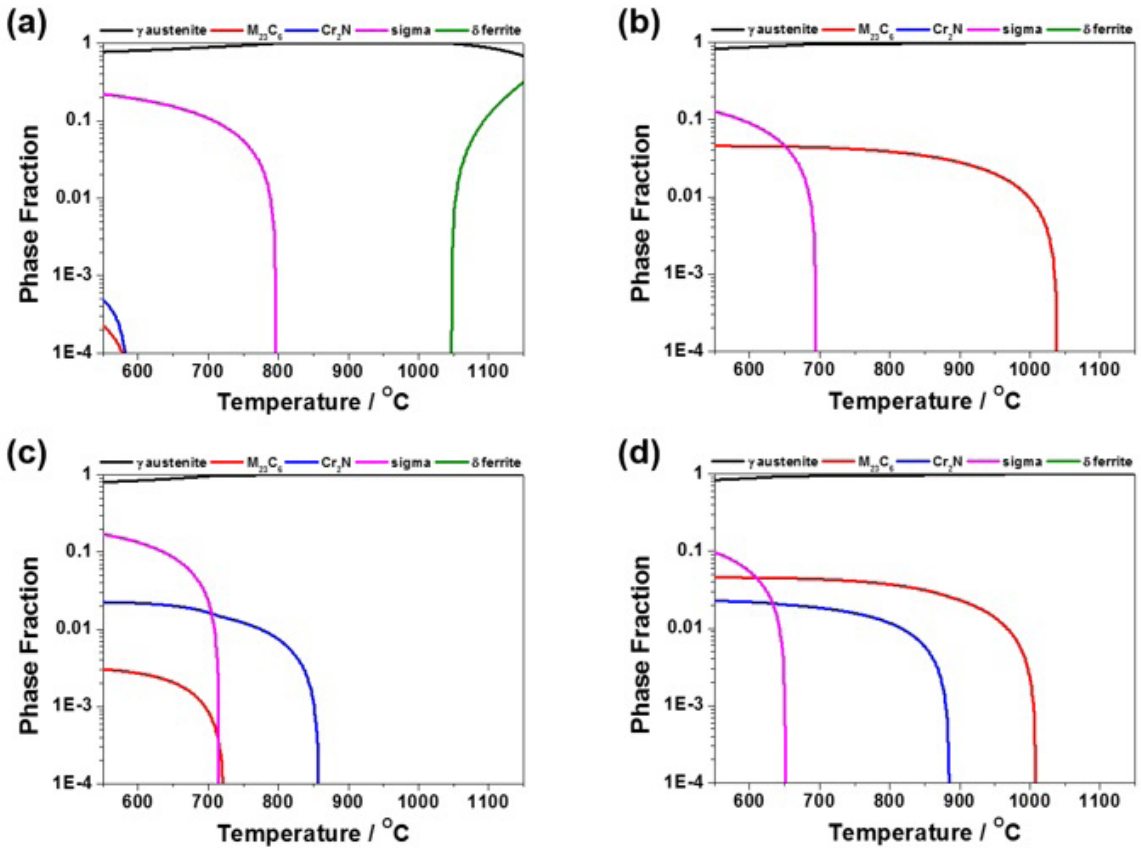


**Fig. 4** - Phase fraction of (a) Base, (b) C2, (c) N2, and (d) CN20. Note that the phase fractions are given in log scale.

In Base, δ-ferrite was observed at all temperature range (Fig. 1a). It seems that the δ-ferrite has formed during heat treatment before hot rolling or during hot rolling process as δ-ferrite is one of the equilibrium phases above 1000 °C (Fig. 2a). δ-ferrite is known to transform into sigma after heat treatment, producing a mixture of ferrite and sigma over the austenitic matrix [9]. Therefore, intergranular sigma phase was formed during the aging process at 600-700 °C. The sigma phase, either from austenite or δ-ferrite, can be easily distinguished from the preexisting delta by their location. Carbides and nitrides were not observed in this alloy because their estimated phase fractions are less than 0.1% (Fig. 1a). Due to a complicated matrix containing both austenite and δ-ferrite, the mechanical properties of Base are not studied.

In C2, $M_{23}C_6$ formed at all temperatures between 600 and 1000 °C (Fig. 1b). This is consistent with the estimated phase fraction in Fig. 4b. $M_{23}C_6$ always began to precipitate at grain boundaries, and spread into inside grains afterwards. Intragranular carbides were formed only at the temperatures over 700 °C. Nitrides did not form because the C2 alloy contains a negligible amount of nitrogen.

N2 showed $Cr_2N$ at grain boundaries after aging under 800 °C, which corresponds to the equilibrium phase fraction (Fig. 4c). However, unlike other alloys, the precipitates were barely observed due to the low density. Carbides were not observed in this alloy because, as indicated in the Fig. 4c, the phase fraction of $M_{23}C_6$ is negligible (< 1%).

Both carbide and nitride are detected in CN20 as in the calculation results in Fig. 4d. The carbides were formed along grain boundaries, and later inside grains. In comparison with C2, the temperature range for the intergranular carbides decreased from 1000 °C to 900 °C, and the formation was delayed under 700 °C. Intragranular carbides were formed only at 800-900 °C after 1440 min of aging. It is clear that the carbide formation is hindered by the introduction of nitrogen, which agrees with the previous studies [10]. Nitrides, on the other hand, were formed faster at 600 °C, and similar in 700-800 °C when compared with N2. Therefore, it seems that carbon promote the nitride formation.

Sigma phase is expected to form more at 600 °C than $M_{23}C_6$, and $Cr_2N$ in the thermodynamic calculation (Fig. 4). In real observation however, they were not found in C2, N2 and CN20. It seems that sigma phase is suppressed by the for-

mation of carbide and nitride.

Precipitate distributions have been obtained for the alloys aged at 800 °C where most precipitates appear (Fig. 1). The size evolutions of precipitates are similar for all C2, N2, and CN20 regardless of precipitate types and locations, as shown in Fig.5. The size of carbides and nitrides increase to about 0.35 μm after 14400 min aging. The carbides formed inside grains also showed similar size as other intergranular precipitates although intragranular carbides always appear later than intergranular ones.

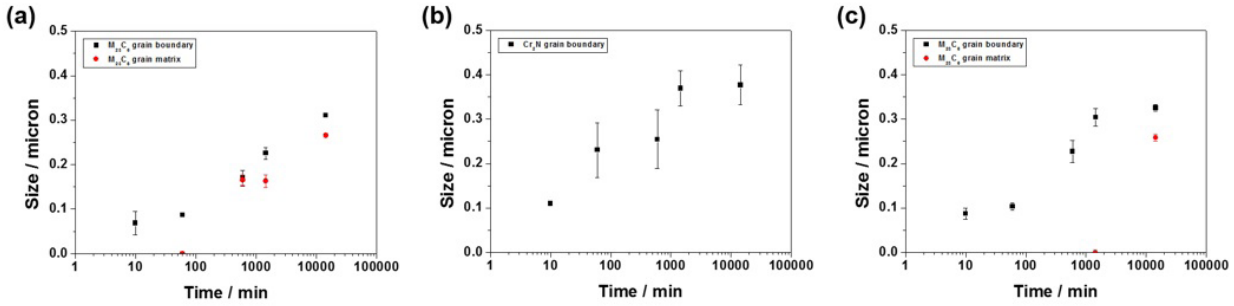


**Fig. 5** - Size change of the precipitates in (a) C2, (b) N2, (c) CN20, with respect to the aging time at 800 °C.

## 2. Tensile behavior

Engineering stress-strain curves of the alloys aged at 800 °C are plotted in Fig. 6, and their yield strength, ultimate tensile strength, and uniform elongation are given in Fig. 7 as a function of the aging time. It is observed that the tensile properties are differently affected by aging at 800 °C depending on the addition of either carbon or nitrogen. Such phenomenon is closely related to the precipitation behavior.

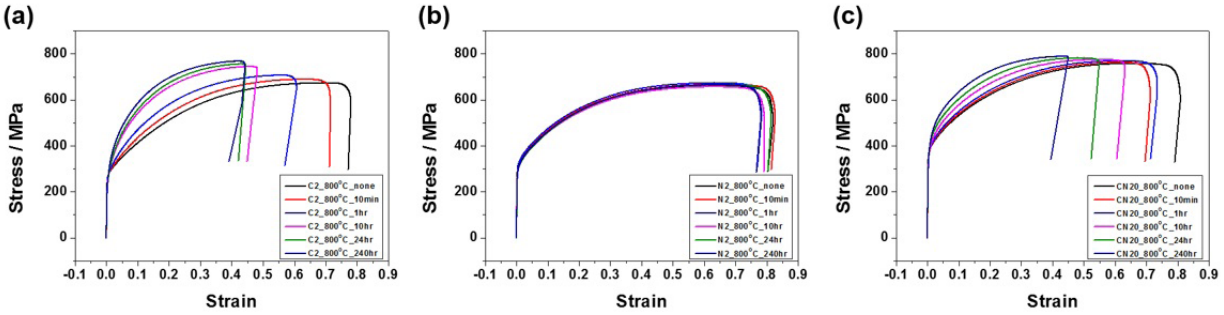


**Fig. 6** - Stress-strain curves of (a) C2, (b) N2, and (c) CN20 aged at 800 °C for different time periods.

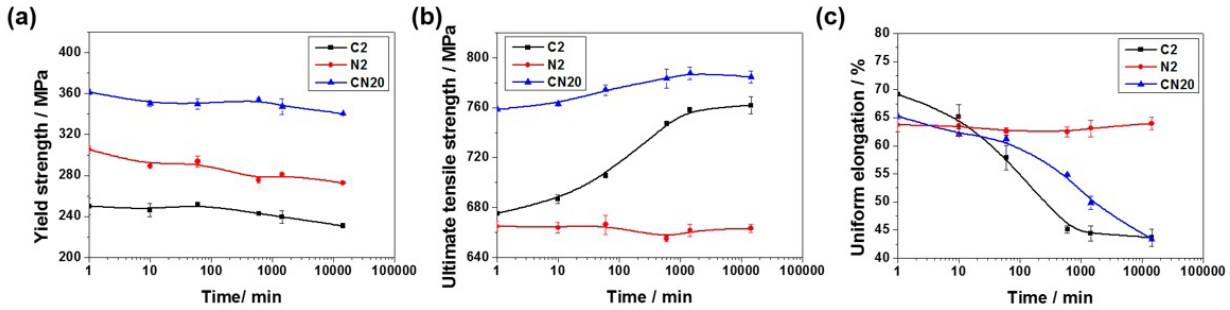


**Fig. 7** - Evolution of (a) yield strength, (b) ultimate tensile strength, and (c) uniform elongation of C2, N2, and CN20 after aging at 800 °C.

Before aging, all carbon and nitrogen atoms are in solid solution for C2, N2, and CN20. As yield strength increases with interstitial contents due to solid solution strengthening, highly alloyed CN20 exhibits the highest yield strength. However, about 50 MPa difference of yield strength exists between C2 and N2 although they have almost the same concentration of interstitial elements ~0.21 wt.% (Table 1). Two factors are most likely to be responsible for such difference: (i) different contributions of carbon and nitrogen to solid solution strengthening, (ii) different grain sizes. Yield strength (YS) of austenitic stainless steels can be estimated by

$$YS(MPa) = 63.5 + 496N + 356.5C + 20.1Si + 3.7Cr + 14.6Mo + 18.6V + 4.5W + 40.3Nb + 26.3Ti + 12.7Al + 2.5\delta + k_{HP} d^{-1/2} \quad (1)$$

where the elements denote their concentration in wt.%, $\delta$ is δ-ferrite content in vol.%, d is the grain size of austenite, and $k_{HP}$ is the Hall-Petch coefficient [11-12]. According to equation (1), the contribution of nitrogen to yield strength is about 1.39 times larger than that of carbon. Considering the carbon and nitrogen concentrations in C2 and N2 (Table 1), the estimated YS difference according to equation (1) is 28 MPa. Moreover, taking $k_{HP}$ = 14.7-23.2 MPa $mm^{-1/2}$ [13], the difference in grain boundary strengthening is 10-14 MPa. By adding the strengthening effects of solid solution and grain boundary, estimated yield strength difference is 38-42 MPa, which explains the difference in the experimental values.

Yield strengths of all three alloys slightly decrease with aging time. Since no change is detected for the grain size of austenite matrix during aging, the yield strength evolution is likely to be related to precipitation strengthening and solid solution strengthening. If precipitation of carbides or nitrides occur during aging, yield strength would increase with aging time due to precipitation strengthening, but it would be reduced by decreasing concentration of interstitials in solid solution, as shown in Fig. 7. Further study is needed to analyze the contribution from each component, and it is being done at the moment.

In order to identify the deformation mechanism, phase maps with twin boundaries of deformed samples without and with aging at 800 °C for 14400 min are shown in Fig. 8. Note that all samples maintained full austenitic microstructure before deformation. It is observed that the fractions of deformation induced ε and α′ martensites are higher in C2 after aging in comparison with C2 without aging. For the unaged samples on the other hand, more deformation twinning is activated (Fig. 8a). However, with aging, precipitates form and the deformation occur with martensite formation. As a consequence, uniform elongation decreases with aging.

In the case of N2, the densities of $Cr_2N$ are much lower although the sizes are similar with carbides (Fig. 5). Thus, the total fraction of $Cr_2N$ formed during aging is too low, and the degree of deformation twinning and deformation induced martensite deformation are similar after aging (Fig. 8b, e). Therefore, both ultimate tensile strength and uniform elongation remains similar with aging.

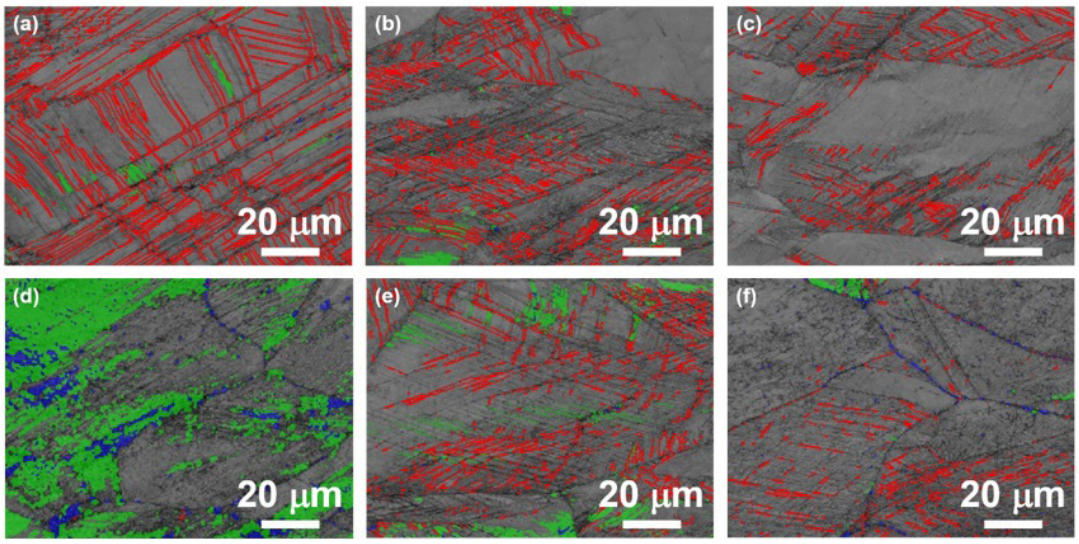


**Fig. 8** - EBSD image of deformed samples, unaged (a) C2, (b) N2, (c) CN20, and aged (d) C2, (e) N2, (f) CN20 at 800 $^{0}$C for 14400 min. Red lines indicate the twin boundaries, green areas are ε-martensite, blue areas are α′-martensite.

In CN20, the formation of carbides are inhibited by nitrogen as in Fig. 2d. Therefore, the deformation twinning activity and deformation induced martensite transformation are not affected as much by aging as those in C2. As a result, the ultimate tensile strength experiences a moderate change with aging (Fig. 7b).

## CONCLUSIONS

1. In the carbon and nitrogen induced 15Cr-15Mn-4Ni austenitic stainless steel, $M_{23}C_6$ carbide and $Cr_2N$ nitride and sigma were precipitated. Alloys containing carbon formed $M_{23}C_6$, ones having nitrogen formed $Cr_2N$, and both carbide and nitride were precipitated together in alloy containing carbon and nitrogen. Carbides were formed with higher density than nitride with greater driving force.

2. Addition of nitrogen hindered the formation of carbide. The temperature range and speed of carbide precipitation were reduced with nitrogen. No distinct change in the kinetics of nitride were observed with adding carbon, although at 600OC, nitride formation was accelerated.

3. Tensile properties were differently affected by aging at 800 $^{0}$C depending on the addition of either carbon or nitrogen. Most changes were observed in C2 with the highest density of precipitates, and N2 had no distinct change in tensile behavior due to low density.

## REFERENCE

[1] V.G. GAVRILJUK, B.D. SHANINA, and H. BERNS, Mater. Sci. Eng. A, 481-482, (2008), p.707.
[2] H.Y. HA, T.H. LEE, C.S. OH, S.J. KIM, Scr. Mater., 61, (2009), p.121.
[3] T.H. LEE, H.Y. HA, S.J. KIM, Metall. Mater. Trans., 42A, (2011), p.3543.
[4] J.W. SIMMONS, Scr. Matall., 32, (1995), p.265.
[5] H. CHANDRA HOLM, P.J. UGGOWITZER, and M.O. SPEIDEL, Scr. Metall., 21, (1987), p.513.
[6] V.G. GAVRILJUK, B.D. SHANINA, and H. BERNS, Acta Mater., 48, (2000), p.3879.
[7] H. BERNS, V.G. GAVRILJUK, S. RIEDNER, and A. TYSHECHENKO, Steel Research. Int., 78, (2007), p.659.
[8] H. BERNS, V.G. GAVRILJUK, and S. RIEDNER, High interstitial stainless austenitic steels, Springer-Verlag Berlin Heidelberg (2013), p. 28
[9] C.C. HSIEH, and W. WU, ISRN Metall., 2012, (2012), 732471
[10] R. PRESSER, J.M. SILCOCK, Metal Sci., 17, (1983), p.241.
[11] V.G. GAVRILJUK, and H. BERNS, High nitrogen steels, Springer-Verlag Berlin Heidelberg (1999), p.136.
[12] K.J. IRVINE, T. GLADMANM, and F.B. PICKERING, JISI, 199, (1969), p.1017.
[13] L.A. NORSTROM, Metal Science, 11, (1977), p.208